

Phenomics data processing: Extracting temperature dose-response curves from repeated measurements

Lukas Roth^{a,*}, Hans-Peter Piepho^b, Andreas Hund^a

^aETH Zurich, Institute of Agricultural Sciences, Universitätstrasse 2, 8092 Zurich, Switzerland

^bUniversity of Hohenheim, Institute for Crop Science, Biostatistics Unit, Fruwirthstrasse 23, 70593 Stuttgart, Germany

Summary

Temperature is a main driver of plant growth and development. New phenotyping tools enable quantifying the temperature response of hundreds of genotypes. Yet, particularly for field-derived data, the process of temperature response modelling bears potential flaws and pitfalls with regard to the interpretation of derived parameters. In this study, climate data from three growing seasons with differing temperature distributions served as starting point for a wheat stem elongation growth simulation, based on a four-parametric Wang-Engel temperature response function. To extract dose-responses from the simulated data, a novel approach to use temperature courses with high temporal resolution was developed. Linear and asymptotic parametric modelling approaches to predict the cardinal temperatures were investigated. An asymptotic model extracted the base and optimum temperature of growth and the maximum growth rate with high precision, whereas simpler, linear models failed to do so. However, when including seasonally changing cardinal temperatures, the prediction accuracy of the asymptotic model was strongly reduced. We conclude that using an asymptotic model based on temperature courses with high temporal resolution is suitable to extract meaningful parameters from field-based data. Consequently, applying the presented modelling approach to high-throughput phenotyping data of breeding nurseries may help selecting for climate suitability.

Keywords: growth, high-throughput field phenotyping, stem elongation, wheat (*Triticum aestivum*).

1. Introduction

Already in 1996, [van Haren](#) noted that the knowledge of crop responses to weather extremes is incomplete and not explicitly included in crop models. Today, high-throughput field phenotyping (HTFP) potentially enables to quantify crop growth—and consequently crop response—of hundreds of genotypes under field conditions ([Araus et al., 2018](#)). Understanding crop responses to environmental factors is essential to secure global food demands: Improvement in wheat yields stagnated on a global scale in the past three decades ([Brisson et al., 2010](#); [Laidig](#)

*Corresponding author: lukas.roth@usys.ethz.ch

28 [et al., 2017](#)). It was suspected that for Europe, the changing climate increasingly impacts wheat yields ([Brisson](#)
29 [et al., 2010](#)). Mitigating these changes in plant breeding to improve yield requires understanding crop responses
30 to environmental factors ([Ramirez-Villegas et al., 2015](#)). A main driver of plant growth and development is
31 temperature ([Porter and Gawith, 1999](#)).

32 *1.1. Approaches to quantify temperature responses under controlled conditions*

33 The effects of changes in temperature on crops are well studied in controlled environments, but the translation
34 of insights to the field is not straightforward. The temperature response of developmental processes is usually
35 studied by exposing plants to different temperature regimes—often during rather short time period of their life
36 cycle. Two different approaches are used: one can either (1) expose different plants of the same genotype
37 to different temperatures ([Slafer and Rawson, 1995](#); [Hund et al., 2012](#); [Reimer et al., 2013](#)), or (2) apply short
38 phases of different temperatures to the same plant. Examples of the latter approach are the studies on leaf growth
39 performed in the indoor platform ‘Phenoarch’, summarized by [Parent and Tardieu \(2012\)](#). This approach requires
40 that the temperature response is measured at a constant growth phase, during which growth is linear when the
41 temperature remains constant. Hence, response-pattern can be observed non-destructively on the same plant,
42 offering a high throughput. In such experiments, the conditions of all but one covariate may be kept constant.
43 Furthermore, the reversibility of the process can be tested by repeatedly applying the same conditions during the
44 course of the experiment.

45 In general, developmental processes follow some sort of peak function in response to increasing temperatures,
46 i.e., there is a base temperature T_{\min} at which growth starts, an optimal temperature T_{opt} at which growth reaches
47 its maximum rate r_{\max} , and a maximum temperature T_{opt} at which growth stops ([Porter and Gawith, 1999](#)).
48 Depending on the research field, different models are used to approximate such functions—for an overview see,
49 e.g., [Wang et al. \(2017\)](#); [Parent et al. \(2019\)](#) for plants, and [Rebaudo et al. \(2018\)](#); [Rebaudo and Rabhi \(2018\)](#) for
50 ectotherms (i.e., animals whose regulation of body temperature depends on external sources). In their work, [Wang](#)
51 [et al. \(2017\)](#) distinguish four types of temperature response functions with increasing complexity. Clearly, type
52 4 functions (linear or curvilinear functions with three cardinal temperatures) are most appropriate to describe
53 temperature responses. Among the most widely used type 4 functions for plants are the Wang-Engel cardinal
54 temperature function ([Wang et al., 2017](#)) and a modified version of the reaction rates equation from [Johnson](#)
55 [et al. \(1942\)](#) applied to different growth processes in a variety of major crops by [Parent and Tardieu \(2012\)](#). We
56 will refer to these different response functions in detail further down.

57 *1.2. Cardinal temperatures of wheat*

58 For wheat, meta-analyses summarizing cardinal temperatures of different developmental processes are to
59 some extent controversial. [Porter and Gawith \(1999\)](#) summarized 65 studies with regard to the minimum (T_{\min}),
60 optimum (T_{opt}) and maximum (T_{\max}) temperature. Mean cardinal temperatures for shoot growth were 3.0 °C
61 (T_{\min}), 20.3 °C (T_{opt}) and > 20.9 °C (T_{\max}). Notably, T_{opt} and T_{\max} were very close together in many studies.

62 In contrast to the comparably low T_{opt} summarized by [Porter and Gawith \(1999\)](#), [Parent and Tardieu \(2012\)](#)
63 reported a significantly higher T_{opt} of 27.7 °C when summarizing 8 studies and own data. We speculate that the
64 discrepancies between the two studies are caused by the fact that the former is based mainly on studies using
65 long-term exposure of individual plants, and the latter on studies that applied short-term changes in temperatures
66 on a growing organ. In the present study we will use the more conservative, i.e., lower, temperature optimum
67 reported by [Porter and Gawith \(1999\)](#).

68 There is evidence that cardinal temperatures are not constant during the lifetime of a crop: [Slafer and Rawson](#)
69 (1995) examined T_{min} and T_{opt} for leaf appearance rates of vernalized winter wheat plants within three phases, i)
70 after vernalization up to the terminal spikelet, ii) from the terminal spikelet up to heading, and iii) from heading
71 to anthesis. The authors found that, averaged across cultivars, T_{min} was -1.9 °C, 1.2 °C and 8.1 °C, while T_{opt}
72 was < 22 °C, 25 °C and > 25 °C for the three different phases, respectively. In addition, the cultivars differed
73 substantially for the two parameters. Consequently, one may assume that particularly the base temperature
74 may change cultivar-specific throughout the season. Nevertheless, the estimates from [Slafer and Rawson \(1995\)](#)
75 of cardinal temperatures and their changes were derived from a controlled environment study. The benefits
76 of controlled environment phenotyping lies in the ability to test a wide range of temperature regimes while
77 keeping other influential factors, such as vapor pressure deficit and light, constant. However, plants usually do
78 not experience such conditions in the field, as discussed by [Slafer and Rawson \(1995\)](#).

79 1.3. Approaches to quantify temperature responses with high-throughput in the field

80 Under field conditions, the temperature regimes are distinctly different from the controlled-environment stud-
81 ies considered so far. The environmental covariates in the field follow an annual and diurnal pattern to which
82 plants adjust their life cycle. HTFP offers the possibility to assess crop growth under such more realistic con-
83 ditions with high temporal and spatial resolution ([Rebetzke et al., 2019](#)). Hence, one can use the temperature
84 course during the season to quantify the genotype-specific temperature responses. Still, such studies are sparse.
85 [Grieder et al. \(2015\)](#) extracted the base temperature and response to increasing temperatures at early growth
86 stages before terminal spikelet formation. The authors were able to extract heritable slopes and intercepts of
87 linear responses. [Kronenberg et al. \(2020a\)](#) were able to extract heritable response traits for the stem elongation
88 phase based on data from three seasons. Again, the authors used linear regressions of growth versus temperature
89 as model. [Kronenberg et al. \(2020a\)](#) argued that the recorded average temperatures in the measuring intervals
90 were well below the optimum temperature of 27.7 °C reported by [Parent and Tardieu \(2012\)](#), which would justify
91 approximating a curvilinear with a linear function. However, the optimum temperature of 20.3 °C summarized
92 by [Porter and Gawith \(1999\)](#) is distinctly lower. Following those results, it is likely that growth reached its op-
93 timum during several hours of the day during their measurement period. Therefore, the extracted temperature
94 response (slope) may be greatly affected by the optimum temperature and maximum growth rate at this temper-
95 ature. Thus, modelling plant response to temperature based on HTFP-derived data bears several challenges, e.g.,

96 the comparably sparse measuring frequency, the unpredictable range of temperatures, the changes of cardinal
97 temperatures during the measuring period, and confounding effects between earliness and seasonal temperature
98 development.

99 *1.4. Research aims*

100 HTFP data are characterized by irregular and long trait measurement intervals but regular and short covariate
101 measurement intervals. Our main research question was how to parameterize genotype-specific temperature
102 response pattern from such HTFP data. Using the stem elongation phase of winter wheat as an example, we aimed
103 to evaluate a new modelling approach with regard to its suitability. Therefore, we simulated the temperature-
104 response in the stem elongation phase using a Wang-Engel response function. The chosen parameters were
105 based on existing literature on cardinal temperatures in winter wheat (Porter and Gawith, 1999; Parent and
106 Tardieu, 2012) and enhanced with realistic temperature recordings of the stem elongation phase at the FIP site
107 (Kronenberg et al., 2020a). To evaluate the strengths and limitations of our approach, we added changing
108 cardinal temperatures, shifts in the start and end of the elongation phase, measurement noise, and spatial field
109 inhomogeneities to our simulation.

110 **2. Background**

111 *2.1. Parametric versus semi-parametric approaches*

112 Semi-parametric approaches (e.g., using P-splines) are often favored to extract traits related to growth pro-
113 cesses from HTFP time series (van Eeuwijk et al., 2019), as they avoid the daunting task of modeling explicitly
114 the—potentially unknown—influence of time-dependent covariate courses. In a previous research, we have
115 shown that semi-parametric approaches are suitable to extract timing of key stages and quantities at defined
116 time points or periods from simulated HTFP data. Those data were generated using a dose-response curve that
117 was unknown to the model being fitted, and corresponding covariate dependencies masked by a “smoothing”
118 part in the model (Roth et al., 2021).

119 In contrast, to extract temperature responses, one cannot avoid modeling a dose-response curve explicitly, as
120 one is interested in its parameters. Consequently, we hereafter propose a parametric approach. Although our
121 focus is on HTFP data, the approach is also directly applicable to indoor platform data, but additionally considers
122 HTFP specific characteristics.

123 In comparison to greenhouse or climate chamber data, HTFP data have two major drawbacks: (i) Field-based
124 measurements are notoriously noisy due to environmental and soil inhomogeneities and measurement errors;
125 (ii) the suitability of measured trait time series and covariate courses to answer a research question depends on
126 the good luck of the scientist to catch a meaningful season. Research in agriculture has already addressed some
127 of these limitations with the development of highly specialized experimental designs and matching statistical
128 analysis. We could already show that following these principles is of advantage for HTFP as well (Roth et al.,

129 2021). For brevity, we therefore focus on the extraction of response traits from time series but refrain from further
130 processing to adjusted genotype means. To allow determining and comparing the performance of non-linear and
131 linear models, we use a simulation that is parametrized based on real field data.

132 2.2. Temperature response functions

133 The linear temperature response model used in [Grieder et al. \(2015\)](#) and [Kronenberg et al. \(2020a\)](#) is defined
134 as

$$r_{\text{linear}}(T) = a \cdot (T - T_{\text{min}}), \quad (1)$$

135 where T is the temperature, a is the slope of the response, and T_{min} the base temperature. Note that such a model
136 causes negative growth rates r for $T < T_{\text{min}}$ and does not include an optimum temperature T_{opt} . Therefore, it
137 is likely that the extracted temperature response (slope) is affected by the optimum temperature and maximum
138 growth rate at this temperature. Additionally, using such a Type 1 response will come to its limitation when data
139 ranges span a whole growing season where temperatures also expand to supra-optimal ranges ([Parent et al.,](#)
140 [2019](#)). In the crop model community, models describing the response to temperature vary widely, but most of
141 them consider an optimum temperature beyond which the growth rate levels off ([Bonhomme, 2000](#); [Parent et al.,](#)
142 [2010](#); [Wang et al., 2017](#)).

143 Arrhenius type functions were shown to adequately describe the dose-response relationship between temper-
144 ature and growth across a wide range of temperatures and species ([Parent et al., 2010](#); [Parent and Tardieu, 2012](#)).
145 However, it was disputed whether this approach allows for a mechanistic interpretation of the different model
146 parameters ([Clavijo Michelangeli et al., 2016](#)). Evidently, research in wheat mainly focused on determining car-
147 dinal temperatures such as the lower and upper base temperature of growth T_{min} and T_{max} and the optimum
148 temperature T_{opt} where the growth rate r is maximal ([Porter and Gawith, 1999](#)). [Wang et al. \(2017\)](#) could
149 show that using the Wang-Engel temperature function ([Wang and Engel, 1998](#)) allows to adequately replace an
150 Arrhenius type functions to describe growth rates using these cardinal temperatures,

$$r_{\text{Wang-Engel}}(T) = r_{\text{max}} \cdot \left(\frac{(2(T - T_{\text{min}})^{\alpha}(T_{\text{opt}} - T_{\text{min}})^{\alpha} - (T - T_{\text{min}})^{2\alpha})}{(T_{\text{opt}} - T_{\text{min}})^{2\alpha}} \right)^{\beta} \quad (2)$$

$$\alpha = \frac{\ln(2)}{\ln((T_{\text{max}} - T_{\text{min}})/(T_{\text{opt}} - T_{\text{min}}))} \quad (3)$$

$$\beta = 1, \quad (4)$$

151 where T is the temperature, r_{max} the maximum growth rate at the temperature optimum T_{opt} , T_{min} the lower
152 base temperature and T_{max} the upper base temperature of growth.

153 The Wang-Engel temperature function is a Type 4 response ([Wang et al., 2017](#)) in regards that it is based on
154 three cardinal temperatures T_{min} , T_{max} and T_{opt} . If aiming to extract genotype-specific cardinal temperatures as
155 well as the maximum growth rate r_{max} from HTFP data, this would require to fit a four-parametric non-linear

156 model with parameters that have interdependent constraints (e.g., $T_{\min} < T_{\text{opt}}$). In our experience, extracting
 157 meaningful parameters by fitting such a model to noisy HTFP data is practically impossible for different rea-
 158 sons, i.e., (i) the optimum temperature T_{opt} and maximum growth rate r_{max} are closely correlated, (ii) for field
 159 experiments performed in target environments (without stress treatments), the maximum temperature T_{max} is
 160 typically outside the range of observed data, and (iii) proximity of cardinal temperatures T_{\min} and T_{opt} may pre-
 161 vent model conversions. Some authors have reacted to these restrictions by fixing one or multiple parameters
 162 and normalizing growth rates (Parent and Tardieu, 2012).

163 As a previously unconsidered alternative, we propose a Type 2 response that integrates an optimum temper-
 164 ature (Wang et al., 2017) to approximate the Arrhenius type functions of Parent and Tardieu (2012) based on an
 165 asymptotic model (Figure 1c),

$$r = r_{\text{max}} \cdot (1 - \exp(-\exp(lrc) \cdot (T - T_{\min}))) \quad (5)$$

$$r_{\text{asym}}(T) = \begin{cases} r, & r > 0 \\ 0, & \text{otherwise} \end{cases}, \quad (6)$$

166 where T is the temperature, r_{max} is the maximum growth rate (and therefore the asymptote of the curve), T_{\min}
 167 the base temperature where the growth rate is zero, and lrc characterizes the steepness of the response as the
 168 natural logarithm (l) of the rate (r) constant (c), thus lrc . The proposed asymptotic model does not consider
 169 a maximum temperature and therefore supra-optimal range, and has no inflection point (Paine et al., 2012). It
 170 requires to fit a three-parametric non-linear model.

171 2.3. Combining irregular and long trait measurement intervals with constant and short covariate measurement 172 intervals

173 Independent of the specific dose-response model, one can describe a phenotype y at time point t (Figure 1a)
 174 as the result of such a dose-response model $r()$ (Figure 1c) dependent on a temperature course T_t (Figure 1b)

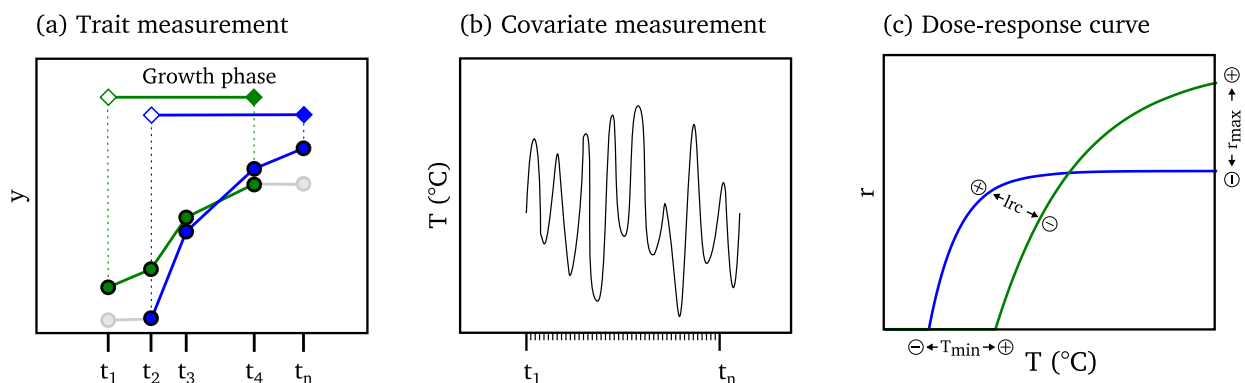


Figure 1: Schematic drawing of trait measurements with irregular and long intervals (a), covariate measurements with short and constant intervals (b), and the asymptotic dose-response model based on a maximum growth rate (r_{max}), minimum temperature (T_{\min}), and steepness of the response (lrc) (c).

175 and a genotype-specific set of crop model parameters θ , e.g., $\theta = (T_{\min}, T_{\text{opt}}, T_{\max}, r_{\max})$,

$$y_t = \int_{t_0}^t r(T_{t'}, \theta) dt', \quad (7)$$

176 where t_0 is the time point where growth started and therefore a timing of key stage trait that needs to be determined
177 beforehand. Trait and covariates such as canopy height and temperatures are only measured at certain points in
178 time, dependent on the measurement interval Δm . We therefore may discretize Equation 7 to

$$y_t = \sum_{t'=t_0}^t r(T_{t'}, \theta) \cdot \Delta m, \quad (8)$$

179 where t' are measurement time points with $(t' = t_0, t_0 + \Delta m, t_0 + 2\Delta m, \dots, t)$, e.g., days.

180 Note that fitting Equation 8 to data implies the same measurement interval for traits y_t and temperatures $T_{t'}$.
181 Although the goal of HTFP is to measure at small measurement intervals, unfavorable weather conditions may
182 prevent regular measurements at all times, while registering covariates is weather-independent and done with
183 constant high frequency. Outdoor phenotyping therefore produces trait measurements with irregular and long
184 measurement intervals Δm_d (e.g., measurements every 3–4 days) but covariate measurements with constant and
185 short measurement intervals Δm_h (e.g., hourly measurements). Therefore, before applying Equation 8 to data,
186 an aggregation step is required.

187 A common technique is to align trait and covariate measurements by aggregating the covariate values to a
188 mean (e.g., [Kronenberg et al., 2017, 2020a](#)),

$$y_t = \sum_{d=t_0}^t (r(\bar{T}_d, \theta) \cdot \Delta m_d), \quad (9)$$

189 where \bar{T}_d is the mean of all covariate measurements made in the time period between successive trait measure-
190 ment time points d where $(d = t_0, t_0 + \Delta m_1, t_0 + \Delta m_1 + \Delta m_2, \dots, t)$. In this study, we propose an alternative
191 approach: One may also apply the dose-response function r to each covariate value T_{dh} where h indexes covariate
192 values between successive trait measurement time points d , $(h = 1, \dots, n_d)$, and sum up the responses to the trait
193 measurements,

$$y_t = \sum_{d=t_0}^t \left(\sum_{h=1}^{n_d} r(T_{dh}, \theta) \cdot \Delta m_h \right). \quad (10)$$

194 In the following, the first method is denoted the T_{mean} method and the second method the T_{course} method.

195 3. Materials and Methods

196 3.1. Simulation of canopy height data

197 The canopy growth of wheat genotypes was simulated using a growth function g_T that was based on the
198 Wang-Engel dose-response model of Equation 4 parameterized with four genotype-specific dose-response crop

199 model parameters $\theta^C = (T_{\min}, T_{\text{opt}}, T_{\max}, r_{\max})$. This model was extended with time points for the start and
 200 end of growth, parameterized with two genotype-specific timing traits $\theta^T = (t\text{PH}_{\text{start}}, t\text{PH}_{\text{stop}})$. An environment
 201 inhomogeneity factor u and a measurement error e were added, leading to the model

$$y_{it} = g_T(t, \theta_i^C, \theta_i^T; T_{dh}) + u_{it} + e_t, \quad (11)$$

202 where y_{it} is the measured canopy height (phenotype) for the i th genotype at campaign time points t in intervals
 203 of three days ($t = 1, 4, 7, \dots, T$), θ_i^C and θ_i^T are genotype-specific crop growth model parameters respectively
 204 timing traits, T_{dh} are hourly (h) temperature readings nested in measurement days (d), u_{it} a time point and
 205 genotype-specific inhomogeneity error (i.e., simulating the influence of other covariates than temperature) and
 206 e_t a time point specific measurement error (i.e., simulating random measurement errors). The growth function
 207 g_T was specified as an implementation of Equation 10 based on the Wang-Engel function of Equation 4,

$$g_T(t, \theta^C, \theta^T; T_{dh}) = \sum_{d=1}^t \begin{cases} \sum_{h=1}^{72} r_{\text{Wang-Engel}}(T_{dh}, \theta^C) & t\text{PH}_{\text{start}} < d < t\text{PH}_{\text{stop}} \\ 0, & \text{otherwise.} \end{cases} \quad (12)$$

208 The genotype-specific traits θ_i^C and θ_i^T and the errors u_{it} and e_{it} were simulated using normal distributions
 209 ($\sim \mathcal{N}(\mu, \sigma^2)$) for genotype traits respectively first order auto-correlations ($\sim \text{AR}_1(\sigma, \rho)$) for the errors. Specific
 210 μ and σ^2 were chosen based on literature if available, and otherwise based on own field data (Roth, 2021).
 211 Corresponding sources and chosen distributions for all simulation input parameter are summarized in Table 1.
 212 Two alternative simulations were performed: One with changing cardinal temperatures with time (indicated with
 213 ‘ \rightarrow ’ in Table 1), and one with fixed cardinal temperatures (set to the mean of changing cardinal temperatures
 214 indicated in Table 1).

215 Canopy growth was simulated for a measurement interval of three days for a period between the 15th of March
 216 and 20th of July based on temperature courses of three years (Figure 2). A total of 1,000 differing genotypes
 217 were assumed, resulting in 3,000 genotype time series. As temperature data source, real weather data of three
 218 consecutive years at the ETH research station of agricultural sciences in Lindau Eschikon, Switzerland (47.449
 219 N, 8.682 E, 556 m a.s.l.) were used.

220 3.2. Extracting dose-response curves

221 To extract the Wang-Engel dose-response curve parameters T_{\min} , T_{opt} and r_{\max} , the linear and asymptotic
 222 growth response models (Equation 1 and 6) were fitted to canopy height data between $t\text{PH}_{\text{start}}$ and $t\text{PH}_{\text{stop}}$ for
 223 two covariate options, T_{mean} based on averaged temperatures between measurements (Equation 9), and T_{course}
 224 based on temperature courses with a period of one hour (Equation 10).

225 Maximum-likelihood optimization was used to fit Equation 9 to a set of t data points, $X_t = (\vec{T}_t, y_t - y_{(t-1)})$.
 226 Fitting Equation 10 to data required modifying the definition of the data set so that $X_t = (\vec{T}_t, y_t - y_{(t-1)})$, where
 227 \vec{T}_t is a vector of covariate readings between trait measurement time points $t - 1$ and t .

Table 1: Model input parameters for the simulation.

	Values	Source
$\theta_i^T \quad \mathcal{N}(\mu, \sigma^2)$	$\mu_{T_{\min}} = 1.5 \rightarrow 9.5 \text{ } ^\circ\text{C}$	Porter and Gawith (1999) (Terminal spikelet→Anthesis)
	$\sigma_{T_{\min}} = 2 \text{ } ^\circ\text{C}$	Assumption
	$\mu_{T_{\text{opt}}} = 10.6 \rightarrow 21 \text{ } ^\circ\text{C}$	Porter and Gawith (1999) (Terminal spikelet→Anthesis)
	$\sigma_{T_{\text{opt}}} = 2 \text{ } ^\circ\text{C}$	Assumption
	$\mu_{T_{\max}} = 30 \rightarrow 35 \text{ } ^\circ\text{C}$	Porter and Gawith (1999) (Anthesis -1/+4 °C)
	$\sigma_{T_{\max}} = 2 \text{ } ^\circ\text{C}$	Assumption
	$\mu_{r_{\max}} = 1.05 \text{ mm h}^{-1}, \sigma_{r_{\max}} = 0.12 \text{ mm h}^{-1}$	Roth (2021)
$\theta_i^{\text{PH}} \quad \mathcal{N}(\mu, \sigma^2)$	2016: $\mu_{t_{\text{PH}_{\text{start}}}} = 108 \text{ d}, \sigma_{t_{\text{PH}_{\text{start}}}} = 2.8 \text{ d}$	Kronenberg et al. (2020a)
	2017: $\mu_{t_{\text{PH}_{\text{start}}}} = 103 \text{ d}, \sigma_{t_{\text{PH}_{\text{start}}}} = 3.0 \text{ d}$	Kronenberg et al. (2020a)
	2018: $\mu_{t_{\text{PH}_{\text{start}}}} = 101 \text{ d}, \sigma_{t_{\text{PH}_{\text{start}}}} = 3.1 \text{ d}$	Roth (2021)
	2016: $\mu_{t_{\text{PH}_{\text{stop}}}} = 165 \text{ d}, \sigma_{t_{\text{PH}_{\text{stop}}}} = 2.5 \text{ d}$	Kronenberg et al. (2020a)
	2017: $\mu_{t_{\text{PH}_{\text{stop}}}} = 162 \text{ d}, \sigma_{t_{\text{PH}_{\text{stop}}}} = 3.5 \text{ d}$	Kronenberg et al. (2020a)
	2018: $\mu_{t_{\text{PH}_{\text{stop}}}} = 158 \text{ d}, \sigma_{t_{\text{PH}_{\text{stop}}}} = 4.0 \text{ d}$	Roth (2021)
$u_{it} \quad \text{AR}(1)$	$\rho = 0.9, \sigma = 0.003 \text{ m d}^{-1}$	Assumption
$e_t \quad \text{AR}(1)$	$\rho = 0.3, \sigma_m = 0.01 \text{ m}$	Roth et al. (2020)

→ connects lower and upper limit of cardinal temperature ramps

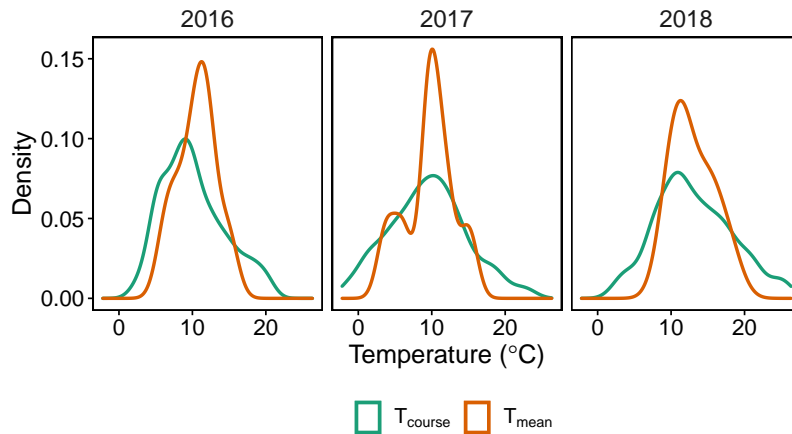


Figure 2: Measured temperatures in the stem elongation phase of winter wheat at the FIP site on an hourly scale (T_{course}) and aggregated to a 3-day scale (T_{mean}).

228 As an independent random measurement errors was assumed, the maximum-likelihood optimization param-
229 eter σ was fixed to the well-known measurement error of the device, herein the simulation input σ_m (Table 1).
230 Parameters were optimized in R using the method L-BFGS-B of the function *optim*.

231 To allow examining the effect of noise caused by inhomogeneities and measurement errors, the extraction
232 was once performed on raw simulated data, once on data contaminated with the measurement error e , and once
233 with both measurement and inhomogeneities errors e and u . Bias, variance, root-mean squared error (RMSE)
234 and Pearson's correlation were calculated after extracting the parameters T_{\min} , lrc and r_{\max} for the asymptotic
235 model and a (slope) and T_{\min} for the linear model.

236 4. Results

237 Aggregating measured temperatures at the FIP site to hourly means (T_{course}) and 3-day means (T_{mean}) revealed
238 sever differences in their distribution (Figure 2): Temperatures close to the cardinal temperatures T_{\min} and T_{opt}
239 were frequent for T_{course} , but almost absent for T_{mean} . Simulating the stem elongation by combining the T_{course}
240 measurements with a Wang-Engel dose-response function resulted in an average final height slightly higher than
241 observed for elite varieties under field conditions (Kronenberg et al., 2020b), but realistic individual plant height
242 time series with characteristic starts, stops, and lag phases (Figure 3). Fitting the asymptotic model based on
243 T_{course} to the simulated data converged for 96% of all genotypes. All other models converged for all genotypes. In
244 a preliminary run, we also tried to fit the Wang-Engel model to simulated data, but failed to extract meaningful
245 parameters. This was partly due to the complexity of defining valid non-overlapping ranges for the cardinal
246 temperatures, but mainly because the model did not converge in most cases.

247 Based on the RMSE, the maximum growth rate r_{\max} and base temperature T_{\min} were best estimated with the
248 asymptotic dose-response model (Equation 5 and 6) based on T_{course} covariates (Table 2). While the variance was
249 drastically lower for both parameters if using T_{course} , the bias slightly increased for r_{\max} but decreased for T_{\min} .
250 The RMSE, bias and variance of the linear model for the parameter T_{\min} was much higher than for the asymptotic
251 model.

252 Introducing a systematic measurement error e did not affect the slope estimated by the linear model; extracted
253 values correlated 1:1 for the simulation with and without noise (Table 3). In contrast, the Pearson's r for T_{\min} was
254 close to zero, but a Spearman's rank correlation revealed nevertheless a high robustness of the extracted ranking
255 to noise. The asymptotic model was more susceptible to noise than the linear model (Table 3). Using temperature
256 courses instead of mean temperatures was of benefit for the parameters r_{\max} and T_{\min} , but of disadvantage for
257 lrc .

258 Correlating simulated versus predicted parameter values revealed further differences between the methods
259 (Figure 4): While the asymptotic model based on T_{course} was able to extract r_{\max} and T_{\min} with very strong
260 correlations to the input values, the same model based on T_{mean} yielded only moderate correlations for r_{\max} and
261 T_{\min} .

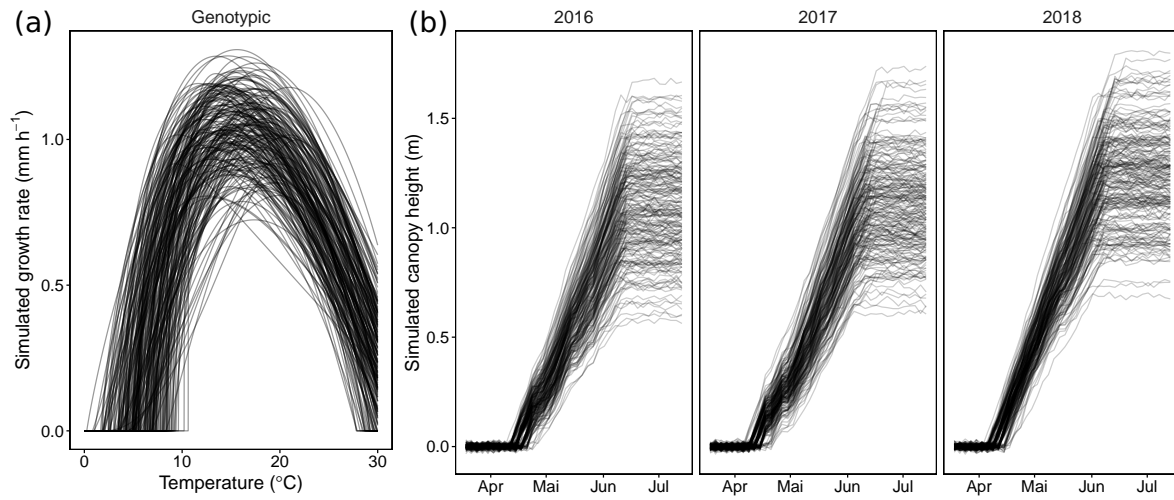


Figure 3: Simulated growth rates (a) and canopy heights (b) for 100 out of 1000 simulated genotypes and three years. Simulated growth rates are based on a Wang-Engel dose-response curve model.

Table 2: Bias, variance and root-mean squared error for the linear and asymptotic model based on mean temperature and temperature courses for simulated data without noise.

Parameter	Model	Bias	Var	RMSE
r_{\max}	Asymptotic T_{mean}	0.0805	0.0347	0.103
	Asymptotic T_{course}	0.0949	0.00309	0.0959
T_{\min}	Linear T_{mean}	9.21	1.96e+08	10.6
	Asymptotic T_{mean}	0.764	2.24	1.04
	Asymptotic T_{course}	-0.352	0.575	0.439
a (slope)	Linear T_{mean}	0.0657	0.00272	0.0657

Table 3: Pearson's and Spearman's correlation between parameters extracted on simulated data with systematic measurement error noise and without noise.

Model	Parameter	Pearson's r	Spearman's r
Linear T_{mean}	a (slope)	1.00	1.00
	T_{\min}	0.00	0.88
Asymptotic T_{mean}	r_{\max}	0.61	0.79
Asymptotic T_{course}	r_{\max}	0.85	0.92
Asymptotic T_{mean}	T_{\min}	0.60	0.66
Asymptotic T_{course}	T_{\min}	0.77	0.72
Asymptotic T_{mean}	lrc	0.69	0.73
Asymptotic T_{course}	lrc	0.46	0.70

Table 4: Bias, variance, root-mean squared error and Pearson's correlation of the asymptotic model based on temperature courses with simulated noise due to measurement errors and field and environment inhomogeneities.

Parameter	Noise	Bias	Var	RMSE	Correlation
r_{\max}	-	0.0949	0.00309	0.0959	0.89
	e	0.0971	0.119	0.114	0.3
	$e + u$	0.0964	0.116	0.113	0.3
T_{\min}	-	-0.352	0.575	0.439	0.92
	e	-0.108	5.55	1.27	0.48
	$e + u$	-0.112	5.67	1.28	0.47

e : systematic measurement error noise
 u : field and environment inhomogeneities

262 The parameter r_{\max} extracted by the asymptotic model based on T_{mean} was not only correlated with the
 263 simulated r_{\max} , but also moderately related to T_{opt} . Using T_{course} reduced this moderate bias for the parameter
 264 estimates of r_{\max} but introduced a new weak bias for the parameter estimates of T_{\min} towards T_{opt} . The asymptotic
 265 model additionally allowed estimating T_{opt} using lrc as proxy with a high correlation to input values.

266 For the linear model, both parameter estimates of slope and T_{\min} were uncorrelated with the corresponding
 267 simulated input parameter (Figure 4b). Instead, the slope was related to r_{\max} , T_{\min} and T_{opt} , while T_{\min} based on
 268 the estimated intercept was not correlated to any input parameter. Both the linear and asymptotic model were
 269 not affected by supra-optimal temperatures: the input parameter T_{\max} that defined growth in the supra-optimal
 270 range above T_{opt} was uncorrelated with any extracted parameter.

271 Adding noise to the simulated growth time series led to increased variances for the parameter estimates of
 272 r_{\max} and T_{\min} based on the asymptotic model (Table 4). While the RMSE drastically increased by a factor of three
 273 for T_{\min} and the correlation to input values dropped below 0.5, it remained low for r_{\max} while the correlation
 274 with input parameter dropped to 0.3. The bias for r_{\max} remained unchanged, while the bias for T_{\min} decreased.
 275 Adding additional noise caused by highly auto-correlated spatial inhomogeneities did not further decrease the
 276 RMSE or increase the variance and bias.

277 Simulating changing cardinal temperatures for all genotypes alike decreased correlations of extracted param-
 278 eters for all models (Figure 4c). The differences between T_{mean} and T_{course} for the asymptotic model disappeared:
 279 While both models were able to extract r_{\max} with moderate correlations, they failed to extract T_{\min} . The curvature
 280 parameter lrc was now moderately correlated with T_{\min} and T_{opt} for T_{mean} and weakly correlated with T_{\min} and
 281 T_{opt} for T_{course} . The slope extracted by the linear model was moderately related to T_{\min} and weakly to r_{\max} and
 282 T_{opt} . Again, T_{\max} was uncorrelated with any extracted parameter.

283 5. Discussion

284 Although the growth of simulated canopies was based on a Wang-Engel temperature dose-response curve,
 285 using a corresponding model to extract parameters turned out to be not suitable, mainly because of failed con-

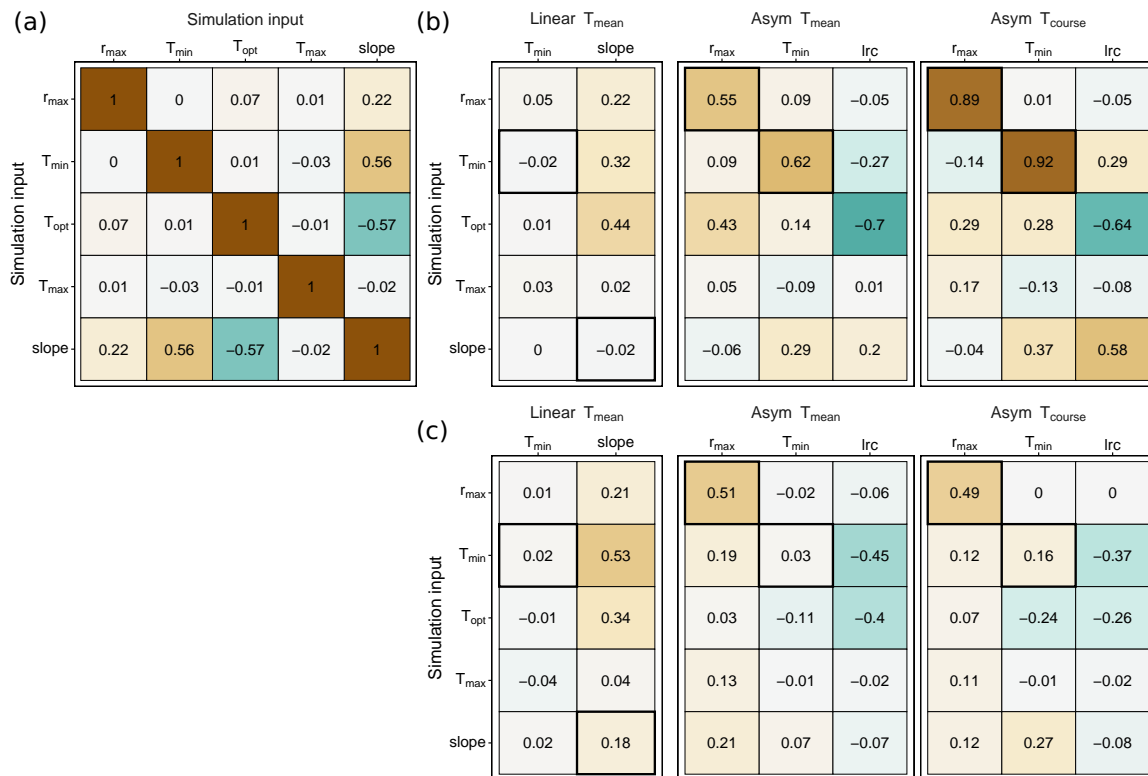


Figure 4: Pearson's correlations of simulated data versus extracted temperature response parameters. Provided are results for the simulation without noise (a) versus extracted temperature response parameters with fixed cardinal temperatures (b) and changing cardinal temperatures with time (c) for the linear model based on mean temperature (Linear T_{mean}) and the asymptotic growth model based on mean temperature (Asym T_{mean}) and temperature courses (Asym T_{course}). Note that the slope is derived from the relation $slope = r_{max}/(T_{opt}-T_{min})$ and therefore not an independent input parameter of the simulation. Black bold boxes indicate correlations between predicted and true values for identical parameters.

286 vergence. Presumably, non-existing measurements at supra optimal temperatures ($\gtrsim 30$ °C, Figure 2) prevented
287 estimating the required parameter T_{\max} . As suspected, the asymptotic model performed better with percentages
288 of converged time series close to 100%. Using temperature courses instead of aggregated mean values allowed es-
289 timating independent parameters with higher correlations to input parameters, to the cost of a slightly decreased
290 convergence rate. Especially the parameter T_{\min} profited from taking temperature courses into account (Table
291 2), which indicates that in the early phase where stem elongation starts the distribution of temperatures and
292 therefore temperature courses are essential to describe temperature responses ($\lesssim 5$ °C, Figure 2). Additionally
293 to T_{\min} , the asymptotic model will extract the maximum growth rate r_{\max} and the parameter lrc which is related
294 to the optimum temperature T_{opt} , and therefore allow to fully describe temperature responses between the lower
295 base temperature T_{\min} and optimum temperature T_{opt} . A limitation of the proposed asymptotic approach may be
296 the high optimum temperatures: Although the extracted base temperature T_{\min} and maximum growth rate r_{\max}
297 were strongly correlated with input parameters, they were also slightly biased by the optimum temperature T_{opt} .

298 Noise and environment inhomogeneities reduced the correlation to input parameters drastically, independent
299 on whether RMSE stayed stable or not (Table 4). It seems reasonable to assume that this reduction in correlation
300 will lead to reduced heritabilities of measured traits in HTPF. The simulation was not including a randomized field
301 experiment set-up, but only independent genotype time series. Nevertheless, we assume based on our previous
302 study on two other intermediate traits (Roth et al., 2021) that also for dose-response curve traits it is essential
303 to follow the three principles of experimental design, i.e., replication, randomization and blocking (Kempton,
304 1984). Such an experimental design will allow to process the extracted plot-based parameters using, e.g., linear
305 mixed models to compensate for measurement errors and environment inhomogeneities and therefore ensure
306 the overall heritability.

307 Simulating changing cardinal temperatures drastically reduced the ability of the asymptotic model to extract
308 meaningful cardinal temperatures (Figure 4c). We suspect that this effect was overamplified by the simulation
309 and that supposed cardinal temperature ramps in Porter and Gawith (1999) may be too extreme for wheat elite
310 cultivar sets. Nevertheless, in the worst case that cardinal temperature ramp assumptions were justified, the
311 asymptotic model would yield less heritable parameters than in the optimum case of fixed cardinal temperatures,
312 but not introduce additional biases.

313 In contrast, one may conclude that using a ‘simple’ linear model to avoid the complexity of curvy dose-
314 response models is not advisable. The results of this study demonstrated that the extracted linear response to
315 temperature (slope) was similarly related to both cardinal temperatures T_{\min} and T_{opt} but also to the maximum
316 growth rate r_{\max} , while unrelated to the simulated slope (Figure 4b). Thus, the apparent temperature response
317 is mainly driven by cardinal temperatures. When fitting a linear model to a wide temperature range, with sig-
318 nificant number of hours in temperature ranges beyond the optimum (Figure 2), it will inevitably compensate
319 for both the maximum growth rate at the optimum and the base temperature of growth. Using a linear model if
320 cardinal temperatures are not fixed is even more harmful: The relation of the slope may switch from T_{opt} towards

321 T_{\min} (Figure 4c). Depending on the examined genetic material, applying a linear model may therefore lead to
322 completely different conclusions. Eventually, one has to review existing literature that refers to slopes as temper-
323 ature responses (e.g., Kronenberg et al., 2020a) being at least partly affected by growth at optimum temperature,
324 maximum growth rate, and changing cardinal temperatures.

325 Using modeling we aimed to simulate different aspects of temperature-response during the important phase
326 of stem elongation of wheat. A major advantage of this approach is that it can be used to test different approaches
327 to parameterize temperature-response. This approach is particularly valuable as other factors such as, e.g., the
328 effect of drying soil, extremely low vapor pressure deficit, or low radiation, do not have to be included. For real
329 field data, such influences will have to be considered to improve the model.

330 6. Conclusion

331 Adequate models to quantify the different aspects of growth response to temperature may greatly improve
332 our understanding of crop adaptation to certain climatic scenarios. Asymptotic models represent a valid choice
333 if sampling winter wheat genotypes in an environment where the decrease in growth after reaching an opti-
334 mum temperature is negligible. Using temperature courses with high temporal resolution as covariate input for
335 the model fit instead of aggregated mean temperatures is advisable. Changing cardinal temperatures—related
336 to advancing phenology—may reduce the ability to extract parameters with an asymptotic model but will not
337 severely bias results. Nevertheless, measurement noise and environment and field inhomogeneities may signifi-
338 cantly increase the variance of extracted parameters. Care should be taken if interpreting existing literature based
339 on linear temperature growth response models, as extracted response reactions may be strongly biased by base
340 and optimum temperature, maximum growth rate at optimum temperature, and changing cardinal temperatures
341 with time. As supra optimal temperatures before flowering are hardly ever reached in a temperate climate, we
342 conclude that models including maximal temperatures will neither deliver any benefit under these conditions.

343 Acknowledgement

344 We like to acknowledge Lukas Kronenberg for feedback on an early version of the manuscript, and Norbert
345 Kirchgessner for feedback on formula notations (both ETH Zurich).

346 Funding

347 LR received funding from Innosuisse (<http://www.innosuisse.ch>) in the framework for the project “Trait
348 spotting” (grant number: KTI P-Nr 27059.2 PFLS-LS). HPP was supported by DFG grant PI 377/24-1.

349 Declaration of Competing Interest

350 The authors declare no conflict of interest.

351 **CRediT authorship contribution statement**

352 **Lukas Roth:** Conceptualization, Methodology, Software, Formal analysis, Visualization, Writing - Original
353 Draft. **Hans-Peter Piepho:** Conceptualization, Methodology, Writing - Review & Editing. **Andreas Hund:** Con-
354 ceptualization, Supervision, Project administration, Funding acquisition, Writing - Review & Editing.

355 **Data availability**

356 Data and source code that support the findings of this study are openly available in the ETH gitlab reposi-
357 tory at https://gitlab.ethz.ch/crop_phenotyping/htfp_data_processing and archived in the ETH
358 research collection (<http://doi.org/10.5905/ethz-1007-385>).

359 References

- 360 José Luis Araus, Shawn C. Kefauver, Mainassara Zaman-Allah, Mike S. Olsen, and Jill E. Cairns. Translating High-Throughput Phenotyping
361 into Genetic Gain. *Trends in Plant Science*, 23(5):451–466, 2018. ISSN 13601385. doi: 10.1016/j.tplants.2018.02.001.
- 362 Raymond Bonhomme. Bases and limits to using ‘degree.day’ units. *European Journal of Agronomy*, 13:1–10, 2000. ISSN 11610301. doi:
363 10.1016/S1161-0301(00)00058-7.
- 364 Nadine Brisson, Philippe Gate, David Gouache, Gilles Charmet, François Xavier Oury, and Frédéric Huard. Why are wheat yields stagnating
365 in Europe? A comprehensive data analysis for France. *Field Crops Research*, 119:201–212, 2010. ISSN 03784290. doi: 10.1016/j.fcr.
366 2010.07.012.
- 367 José A. Clavijo Michelangeli, Thomas R. Sinclair, and Nikolay Bliznyuk. Using an Arrhenius-type function to describe temperature response
368 of plant developmental processes: Inference and cautions. *New Phytologist*, 210(2):377–379, 2016. ISSN 14698137. doi: 10.1111/nph.
369 13812.
- 370 Christoph Grieder, Andreas Hund, and Achim Walter. Image based phenotyping during winter: a powerful tool to assess wheat genetic
371 variation in growth response to temperature. *Functional Plant Biology*, 42:387–396, 2015. ISSN 1445-4408. doi: 10.1071/fp14226.
- 372 Andreas Hund, Regina Reimer, Peter Stamp, and Achim Walter. Can we improve heterosis for root growth of maize by selecting parental
373 inbred lines with different temperature behaviour? *Philosophical Transactions of the Royal Society B: Biological Sciences*, 367:1580–1588,
374 2012. ISSN 14712970. doi: 10.1098/rstb.2011.0242.
- 375 Frank H. Johnson, Hentry Eyring, and R. W. Williams. The nature of enzyme inhibitions in bacterial luminescence: sulfanilamide, urethane,
376 temperature and pressure. *Journal of Cellular and Comparative Physiology*, 20(3):247–268, 1942.
- 377 R.A. Kempton. The design and analysis of unreplicated field trials. *Vorträge für Pflanzenzüchtung*, 7:219–242, 1984.
- 378 Lukas Kronenberg, Kang Yu, Achim Walter, and Andreas Hund. Monitoring the dynamics of wheat stem elongation: genotypes differ at
379 critical stages. *Euphytica*, 213(157), 2017. doi: 10.1007/s10681-017-1940-2.
- 380 Lukas Kronenberg, Steven Yates, Martin P Boer, Norbert Kirchgessner, Achim Walter, and Andreas Hund. Temperature response of wheat
381 affects final height and the timing of stem elongation under field conditions. *Journal of Experimental Botany*, 2020a. doi: 10.1093/jxb/
382 eraa471.
- 383 Lukas Kronenberg, Steven Yates, Shiva Ghiasi, Lukas Roth, Michael Friedli, Michael E. Ruckle, Roland A. Werner, Flavian Tschurr, Melanie
384 Binggeli, Nina Buchmann, Bruno Studer, and Achim Walter. Rethinking temperature effects on leaf growth, gene expression and
385 metabolism: Diel variation matters. *Plant, Cell and Environment*, pages 1–15, 2020b. ISSN 0140-7791. doi: 10.1111/pce.13958.
- 386 Friedrich Laidig, Hans-Peter Piepho, Dirk Rentel, Thomas Drobek, Uwe Meyer, and Alexandra Huesken. Breeding progress, environmental
387 variation and correlation of winter wheat yield and quality traits in German official variety trials and on-farm during 1983–2014. *Theoretical
388 and Applied Genetics*, 130:223–245, 2017. doi: 10.1007/s00122-016-2810-3.
- 389 C. E. Timothy Paine, Toby R. Marthews, Deborah R. Vogt, Drew Purves, Mark Rees, Andy Hector, and Lindsay A. Turnbull. How to fit
390 nonlinear plant growth models and calculate growth rates: An update for ecologists. *Methods in Ecology and Evolution*, 3:245–256, 2012.
391 ISSN 2041210X. doi: 10.1111/j.2041-210X.2011.00155.x.
- 392 Boris Parent and François Tardieu. Temperature responses of developmental processes have not been affected by breeding in different
393 ecological areas for 17 crop species. *New Phytologist*, 194:760–774, 2012. ISSN 0028646X. doi: 10.1111/j.1469-8137.2012.04086.x.
- 394 Boris Parent, O. Turc, Y. Gibon, M. Stitt, and F. Tardieu. Modelling temperature-compensated physiological rates, based on the co-ordination
395 of responses to temperature of developmental processes. *Journal of Experimental Botany*, 61(8):2057–2069, 2010. ISSN 00220957. doi:
396 10.1093/jxb/erq003.
- 397 Boris Parent, Emilie J. Millet, and François Tardieu. The use of thermal time in plant studies has a sound theoretical basis provided that
398 confounding effects are avoided. *Journal of Experimental Botany*, 70(9):2359–2370, 2019. ISSN 14602431. doi: 10.1093/jxb/ery402.
- 399 John R. Porter and Megan Gawith. Temperatures and the growth and development of wheat a review. *European Journal of Agronomy*, 10:
400 23–36, 1999. doi: 10.1016/S1161-0301(98)00047-1.
- 401 Julian Ramirez-Villegas, James Watson, and Andrew J. Challinor. Identifying traits for genotypic adaptation using crop models. *Journal of
402 Experimental Botany*, 66(12):3451–3462, 2015. ISSN 14602431. doi: 10.1093/jxb/erv014.
- 403 François Rebaudo and Victor Badre Rabhi. Modeling temperature-dependent development rate and phenology in insects: review of major
404 developments, challenges, and future directions. *Entomologia Experimentalis et Applicata*, 166:607–617, 2018. ISSN 15707458. doi:
405 10.1111/eea.12693.
- 406 François Rebaudo, Quentin Struelens, and Olivier Dangles. Modelling temperature-dependent development rate and phenology in arthropods:
407 The devRate package for R. *Methods in Ecology and Evolution*, 9:1144–1150, 2018. ISSN 2041210X. doi: 10.1111/2041-210X.12935.
- 408 G. J. Rebetzke, J. Jimenez-Berni, R. A. Fischer, D. M. Deery, and D. J. Smith. Review: High-throughput phenotyping to enhance the use of
409 crop genetic resources. *Plant Science*, 282:40–48, 2019. doi: 10.1016/j.plantsci.2018.06.017.
- 410 Regina Reimer, Benjamin Stich, Albrecht E. Melchinger, Tobias A. Schrag, Anker P. Sørensen, Peter Stamp, and Andreas Hund. Root response
411 to temperature extremes: Association mapping of temperate maize (*Zea mays* L). *Maydica*, 58:156–168, 2013. ISSN 22798013.
- 412 Lukas Roth. *Development of drone-based phenotyping methodologies to support physiological plant breeding of wheat and soybean*. PhD thesis,
413 mar 2021. URL <https://www.research-collection.ethz.ch/443/handle/20.500.11850/474271>.
- 414 Lukas Roth, Moritz Camenzind, Helge Aasen, Lukas Kronenberg, Christoph Barendregt, Karl-Heinz Camp, Achim Walter, Norbert Kirchgessner,
415 and Andreas Hund. Repeated Multiview Imaging for Estimating Seedling Tiller Counts of Wheat Genotypes Using Drones. *Plant Phenomics*,
416 2020(3729715), 2020. doi: 10.34133/2020/3729715.
- 417 Lukas Roth, María Xosé Rodríguez-Álvarez, Fred van Eeuwijk, Hans-Peter Piepho, and Andreas Hund. Phenomics data processing: A
418 plot-level model for repeated measurements to extract the timing of key stages and quantities at defined time points. *bioRxiv*, page
419 2021.05.02.442243, jan 2021. doi: 10.1101/2021.05.02.442243.
- 420 Gustavo A. Slafer and H. M. Rawson. Rates and cardinal temperatures for processes of development in wheat: Effects of temperature and
421 thermal amplitude. *Australian Journal of Plant Physiology*, 22:913–926, 1995. ISSN 03107841. doi: 10.1071/PP9950913.
- 422 Fred A. van Eeuwijk, Daniela Bustos-Korts, Emilie J. Millet, Martin P. Boer, Willem Kruijer, Addie Thompson, Marcos Malosetti, Hiroyoshi

- 423 Iwata, Roberto Quiroz, Christian Kuppe, Onno Muller, Konstantinos N. Blazakis, Kang Yu, Francois Tardieu, and Scott C. Chapman.
424 Modelling strategies for assessing and increasing the effectiveness of new phenotyping techniques in plant breeding. *Plant Science*, 282:
425 23–39, 2019. ISSN 18732259. doi: 10.1016/j.plantsci.2018.06.018.
- 426 R. van Haren. Evaluation of crop production sensitivity to weather extremes. Workplan Document of the Research Institute for Agrobiolgy
427 and Soil Fertility and the C.T. de Wit Graduate School for Production Ecology. Technical report, 1996.
- 428 Enli Wang and Thomas Engel. Simulation of phenological development of wheat crops. *Agricultural Systems*, 58(1):1–24, 1998. ISSN
429 0308521X. doi: 10.1016/S0308-521X(98)00028-6.
- 430 Enli Wang, Pierre Martre, Zhigan Zhao, Frank Ewert, Andrea Maiorano, Reimund P Rötter, Bruce A. Kimball, Michael J. Ottman, Gerard W.
431 Wall, Jeffrey W. White, Matthew P Reynolds, Phillip D. Alderman, Pramod K. Aggarwal, Jakarat Anothai, Bruno Basso, Christian Biernath,
432 Davide Cammarano, Andrew J. Challinor, Giacomo De Sanctis, Jordi Doltra, Elias Fereres, Margarita Garcia-Vila, Sebastian Gayler, Gerrit
433 Hoogenboom, Leslie A. Hunt, Roberto C. Izaurralde, Mohamed Jabloun, Curtis D. Jones, Kurt C. Kersebaum, Ann Kristin Koehler, Leilei Liu,
434 Christoph Müller, Soora Naresh Kumar, Claas Nendel, Garry O’Leary, Jørgen E. Olesen, Taru Palosuo, Eckart Priesack, Ehsan Eyshi Rezaei,
435 Dominique Ripoche, Alex C. Ruane, Mikhail A. Semenov, Iurii Shcherbak, Claudio Stöckle, Pierre Stratonovitch, Thilo Streck, Iwan Supit,
436 Fulu Tao, Peter Thorburn, Katharina Waha, Daniel Wallach, Zhimin Wang, Joost Wolf, Yan Zhu, and Senthold Asseng. The uncertainty
437 of crop yield projections is reduced by improved temperature response functions. *Nature Plants*, 3(17102), 2017. ISSN 20550278. doi:
438 10.1038/nplants.2017.102.